International Journal for Housing Science and Its Applications
Publish August 10, 2025. Volume 46, Issue 4 Pages 7356-7369

https://doi.org/10.70517/ijhsa464637

Optimizing Hospital Space Layout for Patient Safety and Building a Pathway for Clinical Risk Management Coordination

Xiaojun Wang[1,*]
[1] The Second People's Hospital of Yangquan City, Yangquan, Shanxi, 045000, China
Corresponding authors: (e-mail: running2049558@126.com).

Abstract To adapt to advancements in medical technology and the growing demand for healthcare services, and in response to national policies regarding hospital capacity expansion and improvements in medical service capabilities, it is necessary to optimize and renovate hospital spatial layouts. This article establishes a hospital spatial layout optimization model based on the patient safety accessibility gravity model, with the objectives of enhancing patient safety assurance capabilities and risk management capabilities. Using AnyLogic software, a simulation model and spatial layout optimization strategies were developed. An improved sparrow search algorithm is then introduced to optimize the parameters of the GRU model, thereby solving the optimization model and predicting clinical risks. A simulation analysis is conducted using a certain hospital as the research object. The study shows that the ISSA-GRU model has good solution and prediction performance, and the application of spatial layout optimization strategies can significantly reduce the passenger density, waiting time, and infection risk in the hospital waiting area, providing a reliable guarantee for improving the safety level of the patient's medical environment.

Index Terms spatial layout optimization model, AnyLogic, improved sparrow search algorithm, GRU model

I. Introduction

In recent years, with the rapid development of the economy and society, the process of urbanization has accelerated, and population mobility and concentration have become increasingly prominent. This trend has highlighted the irrational allocation of public resources, particularly in the spatial layout of public service facilities (such as education, healthcare, and emergency services), which directly impacts the quality of life of the public and the harmony and stability of society [1]-[3]. Hospitals, as a core component of the healthcare system, play a crucial role in the design of medical institutions. Their spatial distribution affects the efficiency of medical staff, communication and interaction between medical staff and patients, and the patient experience. The rationality of their spatial layout not only impacts the accessibility and fairness of healthcare services but also directly affects public health safety and emergency response efficiency [4]-[8].

Some scholars have conducted research on the spatial layout of hospitals. Reference [9] developed a low-trust social force model, constructing a simulation model based on medical process analysis, hospital spatial surveys, and infection theory. The model simulated spatial layouts before and after hospital planning, obtained key local indicators, and visualized multiple spatial layout planning schemes. By combining LISFM (Lateral Inversion Spin-Filter Magnetoresistance) computer simulations, the optimal spatial layout was planned, reducing overall infection risks while improving service levels. Reference [10] adopts a patient flow-oriented approach with the goal of minimizing patient travel distances. It comprehensively considers relocation costs, local building codes and regulations, functional continuity, and design flexibility. Using optimal path planning and genetic algorithms, it performs hospital layout optimization under computer-aided design. The method improves the spatial proximity, connectivity, and flow resistance of the hospital layout. Reference [11] proposes an environmental performance optimization parametric planning program and applies it to the optimization of comprehensive hospital layout design, thereby improving functional efficiency and reducing energy consumption in the layout space. Reference [12] shares an architect-friendly parametric design combining genetic algorithms and automated machine learning for optimizing hospital interior spatial layout, integrating patient spatiotemporal distribution and natural ventilation conditions, with parameter optimization to reduce infection risks. However, current layouts are limited to rectangular spaces and do not consider irregular spaces.

As the healthcare industry continues to develop, hospitals inevitably face internal and external risks that will not disappear with medical progress [13]. Global patient safety incidents are on the rise, and tensions between patients and healthcare providers are escalating. In an environment where public health awareness, rights protection awareness, and legal system development are increasingly robust, the risks borne by the healthcare industry are growing [14], [15]. How to reduce the occurrence of clinical errors and disputes has become a key focus for managers. Clinical risk management involves a series of proactive, management-oriented professional activities such as identification, assessment, response, and monitoring to minimize clinical risks, prevent or reduce medical disputes, and mitigate economic losses and reputational damage to healthcare institutions, thereby ensuring the smooth achievement of organizational objectives [16], [17]. Establishing a comprehensive, systematic risk management system throughout the entire process can truly reduce the incidence of clinical risk damage and ultimately significantly improve patient safety. Literature [18] points out that the layout and space of outpatient oncology treatment areas affect patient safety through the visibility of communication between clinical doctors during chemotherapy infusion. It is evident that in clinical work, it is necessary to pay attention to hospital spatial layout to reduce clinical risks and enhance patient safety.

Traditional hospital spatial layout optimization methods have certain advantages when addressing small-scale, low-complexity optimization problems. However, as problem scale increases and objective functions and constraints become more complex, the limitations of traditional methods gradually become apparent. This paper focuses on patient safety in hospitals, establishing a hospital spatial layout optimization model with patient safety assurance capabilities and risk management capabilities as objectives. Using AnyLogic software, a spatial layout optimization strategy was designed for a specific hospital. An improved sparrow search algorithm was then used to optimize the parameters of the GRU model, and an ISSA-GRU model was constructed for clinical risk prediction. The effectiveness of the methods proposed in this paper was evaluated through simulation experiments and quantitative data analysis.

II. Hospital space layout optimization model and strategy

Since the beginning of the 21st century, with the increase in residents' demand for medical services, hospital construction has accelerated at an unprecedented rate. However, the lack of control over medical space by urban managers has led to the long-term uncontrolled expansion of medical space, resulting in disorderly and unsustainable development of medical buildings. This traditional “top-down” planning method primarily relies on regulations and indicators, yet ignores the actual needs of patients seeking medical care. Based on this, hospital spatial layout optimization is being conducted to address the safety needs of patients seeking medical care.

II. A. Design of a hospital space layout optimization model

II. A. 1) Patient Safety Accessibility Model

Accessibility is one of the key factors in hospital services. Considering the maximum capacity of hospitals, the distance between patients and hospitals, and other influencing factors, an improved patient safety space accessibility gravity model is proposed based on the gravity model. Let a_{ij} represent the spatiotemporal accessibility of patients in subregion (i,j), which can be expressed as:

$$a_{ij}=\begin{cases}\sum_{k\in K}\eta_1\dfrac{q_{k,\max}\bar{v}_{ijk}}{\bar{d}_{ijk}} & \bar{d}_{ijk}\le d_{k,\max}\\ 0 & \bar{d}_{ijk}>d_{k,\max}\\ \forall i\in N_1, j\in N_2 & \end{cases} \tag{1}$$

In the equation, $K=\{1,2,3,\cdots,k-1,k,k+1,\cdots,k_1-1,k_1\}$ denotes the set of hospitals, $q_{k,\max}$ (number of visits per day) and $d_{k,\max}(km)$ represent the maximum patient care capacity and maximum service coverage radius of the k th hospital, respectively, $\bar{d}_{ijk}(km)$ and $\bar{v}_{ijk}(km/h)$ represent the average distance and average speed from region (i,j) to the k th hospital, respectively. η_1 is a constant representing the correction coefficient for other influencing factors such as population and economy. The smaller the population or the higher the economic level, the larger the value of η_1. $N_1=\{1,2,3,\cdots,i-1,i,i+1,\cdots,n_1-1,n_1\}$ and $N_2=\{1,2,3,\cdots,j-1,j,j+1,\cdots,n_2-1,n_2\}$ represent the sets of location numbers i and j, respectively. The above equation indicates that the patient's safety accessibility is affected by the actual time required to travel from region (i,j) to the hospital.

In this regard, the patient's safety spatiotemporal accessibility A can be expressed as:

$$A = \frac{\sum_{i=1}^{n_1}\sum_{j=1}^{n_2} w_{ij} \cdot a_{ij}}{\sum_{i=1}^{n_1}\sum_{j=1}^{n_2} W_{ij}} \tag{2}$$

In the equation, w_{ij} and W_{ij} represent the actual patient flow and demand within subregion (i, j), respectively. The above equation shows that patient spatiotemporal accessibility A is related to the total patient demand and actual flow, and is influenced by the accessibility of each region.

II. A. 2) Spatial layout optimization model

The optimization of hospital spatial layout is influenced by numerous factors, with patient safety assurance capabilities and risk management capabilities being the two most significant factors, which can be treated as a multi-objective optimization problem. Therefore, based on the patient safety accessibility gravity model, this paper selects resident patient safety assurance capabilities and risk management capabilities as the objective function. Based on the model assumptions, the hospital spatial layout optimization model can be expressed as:

$$Z_1 = \min \sum_{i \in I}\sum_{q \in Q} \frac{d_{ig} n_q^{fun} \delta_{iq}}{\lambda_{\sec} v} \tag{3}$$

$$Z_2 = \min \sum_{i \in I}\sum_{q \in Q} w_{\sec} n_q^{fun} \delta_{iq} b_i \tag{4}$$

s.t.

$$\sum_{q \in Q}\sum_{i \in I} \delta_{iq} \le N_A + N_B \tag{5}$$

$$\sum_{i \in I}\sum_{q \in Q} \delta_{iq} n_q^{fun} \ge n_{all} \tag{6}$$

$$\sum_{q \in Q} \delta_{iq} \le 1 \; \forall i \in I \tag{7}$$

$$\left| x_i - x_j \right| \ge \frac{L_k + L_j}{2} + \Delta x_{kj}, \forall k \ne j \tag{8}$$

$$\left| y_k - y_j \right| \ge \frac{W_k + W_j}{2} + \Delta y_{kj}, \forall k \ne j \tag{9}$$

$$K = \{1, 2, 3, \cdots, N_A + N_B\}, k \in K, j \in K \tag{10}$$

$$\delta_{iq} = \begin{cases} 1 & if\ a\ facility\ of\ type\ q\ is\ constructed\ at\ po\text{int}\ i \\ 0 & else \end{cases} \tag{11}$$

$$b_i = \begin{cases} 1 & if\ \min\{d_{ih}\} \le R \\ 0 & else \end{cases} \tag{12}$$

$$I = \{ i \mid i = 1, 2, 3, \cdots, n_1 \} i \in I \tag{13}$$

$$H = \{ h \mid h = 1, 2, 3, \cdots, n_2 \} h \in H \tag{14}$$

$$Q = \{A, B\} q \in Q \tag{15}$$

In the equation, Z_1 represents the time required to reach the waiting area within the hospital, I denotes the set of hospital facility deployment points, Q denotes the set of hospital facility types, d_{ig} denotes the Euclidean distance from potential hospital facility deployment point i to waiting area g, and n_q^{fun} denotes the number of people that hospital facility type q can accommodate. δ_{iq} is an integer independent variable with values of 0 or

1, $\lambda_{\sec}$ denotes the conversion coefficient for personnel speed under different scenarios, which is related to the regional environment, and v denotes the personnel assembly speed. Z_2 denotes the number of people at clinical risk, $w_{\sec}$ denotes the functional conversion coefficient for q -type facilities under different scenarios, and b_i is an integer independent variable taking values of 0 or 1. N_A and N_B represent the number of Type A and Type B hospital facilities, respectively, n_{all} denotes the scale of hospital personnel, (x_k, y_k) and (x_j, y_j) are the coordinates of facilities k and j , respectively, L_k and W_k denote the length and width of facility k , respectively, L_j and W_j represent the length and width of facility j , respectively. Δx_{kj} and Δy_{kj} represent the minimum horizontal and vertical distances between facilities k and j , respectively, and K represents the waiting time at hospital facilities.

II. B.Spatial layout optimization based on AnyLogic

II. B. 1) AnyLogic Simulation Method

AnyLogic is a tool for hybrid system modeling and simulation. By constructing a pedestrian library and building environment, and adjusting relevant parameters (such as patient arrival rate, number of service counters, and service speed), multiple simulations can be run to determine metrics such as the number of people in the hall and personnel density. AnyLogic, meaning "any logic," can simulate any field with logical structure. Therefore, the application scope of AnyLogic simulation models is extremely broad. From a micro perspective, it can simulate events with precise time, speed, and distance. From a macro perspective, it can simulate dynamic feedback involving dynamic systems, long-term trends, and strategic decisions.

When creating a simulation environment for hospital spatial layout, multiple environmental modules must be considered, such as staircases, elevators, walls, and service areas. To construct these modules, corresponding graphics must be customized and imported into the model library. These graphic objects can be configured with animation properties as needed to more realistically simulate actual conditions. AnyLogic software allows users to customize scales according to specific requirements, thereby creating environment models that better align with actual proportions.

In terms of simulating patient behavior, AnyLogic offers customizable flowchart functionality. By defining object properties based on behavior library modules, users can specify patient behavioral characteristics. These properties may include walking speed, arrival rates, and dwell times. By connecting the various behavior modules via connectors and mapping them to spatial marker modules, accurate behavior simulation can be achieved in the simulated environment.

AnyLogic software typically simplifies patients with different behaviors into two-dimensional planar prototypes of intelligent agents of different colors. On one hand, this facilitates observing patient flow relationships, and on the other hand, it aids in statistically determining the number of patients within a specified range, such as the maximum number of people in the hall in this study. Additionally, the two-dimensional plane can be converted into three-dimensional modeling, making the simulation model more conducive to observation.

II. B. 2) Spatial layout optimization strategies

The primary objective of the AnyLogic experiment is to calculate the number of people that hospital spaces must accommodate, specifically the critical data point of peak waiting room occupancy. Based on this, the experiment aims to quantify the area of the waiting zone and propose more scientifically sound optimization strategies. The AnyLogic experiment process involves: building the model → setting parameters → running the model to generate output data → proposing and validating spatial optimization solutions. For simplicity, the experiment assumes that patient calls are processed in order and that each doctor's service efficiency is roughly equivalent, thereby reducing modeling complexity.

(1) Build the model and set parameters. Import the waiting area layout diagram into AnyLogic and mark the relevant elements of the environmental model, including walls, entrances/exits, key areas (registration area, waiting area, consultation area), services (registration, consultation), and facilities (self-service registration machines, seating areas).

Set up the waiting process model based on patient behavior: Patient source (entering from the entrance) → Scan code for registration (registration area) → Waiting (waiting area) → Consultation (consultation area) → Departure (heading toward the exit) → Patient source dissipates (clear patient source), and set the experimental parameters.

(2) Run the experiment and output the results. Since the specific arrival times of patients are randomly distributed, set the experiment to run 30 times, each lasting 300 minutes (i.e., the morning working hours), to obtain results that

better reflect actual conditions. Through the experiment, the number of waiting patients during peak hours (the critical interval of sharp increases and decreases) can be calculated, and by including the accompanying rate, the number of people in the hall during peak hours can be determined.

Based on the average of the maximum number of people during peak hours, the number of people the waiting area must accommodate is determined. Based on the average of the maximum value and the average of the average value, the recommended seat counts for two comfort levels are determined. The recommended number of seats for the basic comfort level (where the number of seats reaches the average peak period number, meeting the seating needs of most people during most periods) and the recommended number of seats for the special comfort level (where the number of seats reaches the maximum peak period number, meeting the seating needs of all people during all periods).

III. Clinical risk prediction model based on ISSA-GRU

A rational functional layout is a critical component of medical building planning and design, serving as the foundation for the implementation of medical processes. It is the key determinant of whether a medical building can operate efficiently and whether patients can receive care effectively. As the medical system continues to evolve, the functions of medical buildings have also become increasingly diverse, transitioning from single-purpose diagnostic and treatment facilities to comprehensive medical service systems that integrate diagnosis, prevention, and rehabilitation, thereby transforming from “hospitals” into “medical centers.” A functional layout established based on logical relationships can serve as a breakthrough for improving spatial efficiency, enabling patients to receive positive feedback during their visits.

III. A. GRU and Simulated Annealing Algorithm

III. A. 1) Gate Control Cycle Unit

In the computation of gated recurrent unit (GRU) neural networks, gradient explosion and decay occur when there are differences in the number of time steps. Gradient explosion can be resolved through clipping, but gradient decay cannot be addressed. Therefore, gated recurrent units are better suited for capturing distant dependencies in time series data. The design of the gated recurrent unit incorporates two new gating units: the reset gate and the update gate. The reset gate captures short-term dependencies in the array, while the update gate captures long-term dependencies in the array. This modifies the computation method of the recurrent neural network in the hidden state [19]. Figure 1 shows the structure of the GRU recurrent unit.

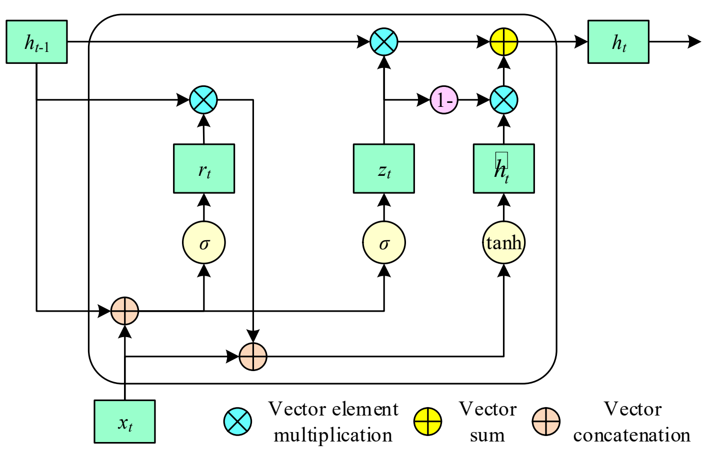

Figure 1: Structure of GRU recirculation un

Recurrent neural networks are simpler than traditional neural networks. GRUs do not introduce additional memory units. The principle of GRU networks can be expressed as follows:

$$h_t = h_{t-1} + g\left(x_t, h_{t-1}; \theta\right) \tag{16}$$

In the equation, h_t is the hidden state passed to the next moment, h_{t-1} is the hidden state of the previous moment, and x_t is the input at moment t.

Based on equation (16), an update gate is introduced to control how much information is retained from the history and how much information is accepted from the candidate states. That is:

$$h_t = z_t \cdot h_{t-1} + (1 - z_t) \cdot g(x_t, h_{t-1}; \theta) \tag{17}$$

$$z_t \in (0,1) \tag{18}$$

$$z_t = \sigma(W_z x_t + U_z h_{t-1} + b_z) \tag{19}$$

In the equation, z_t is the update gate, σ is the sigmoid function, and W and U are weights.

When $z_t = 0$, the relationship between the current state h_t and the previous state h_{t-1} is a functional relationship; when $z_t = 1$, the relationship between h_t and h_{t-1} is a linear functional relationship. That is:

$$g(x_t, h_{t-1}; \theta) \tag{20}$$

$$\tilde{h} = \tanh\left(W_k x_t + U_k (r_t \cdot h_{t-1}) + b_k\right) \tag{21}$$

In the equation, $\tilde{h}$ is the candidate hidden state.

The reset gate can be expressed as:

$$r_t = \sigma(W_r x_t + U_r h_{t-1} + b_r) \tag{22}$$

When $r_t = 0$, the candidate state $\tilde{h}_t = \tanh(Wcxt + b)$ is only related to the current input x_t and is unrelated to the historical state; When $r_t = 1$, the candidate state $\tilde{h}_t = \tanh(Whxt + Uhh_{t-1} + b_k)$ is only related to the current input x_t and the historical state h_{t-1}, consistent with the recurrent network [20].

Therefore, the state update method of the GRU network is:

$$h_t = z_t \cdot h_{t-1} + (1 - z_t) \cdot \tilde{h}_t \tag{23}$$

III. A. 2) Sparrow Search Algorithm

Predatory and anti-predatory behaviors of sparrow groups In this model, individuals in a sparrow group are divided into three roles:

(1) Explorers have the highest fitness value and lead the group in searching for food, discovering potential food sources, and guiding other members to them.

(2) Followers closely monitor the actions of explorers and follow them to the discovered food sources. By following explorers, followers can access better food sources, thereby increasing their fitness values.

(3) Warners issue alerts when danger is detected to protect the entire group. When a warning signal is issued, sparrows in the group quickly move toward safe areas or gather closer to other sparrows to enhance their safety.

The Sparrow Search Algorithm (SSA) is applied to optimization problems. If there are N sparrows in a D-dimensional search space, the position of the i th sparrow in the space is $X_i = [x_{i1}, \cdots, x_{id}, \cdots, x_{iD}]$, and the corresponding fitness value is:

$$F_x = [f(x_{i1}), \cdots, f(x_{id}), \cdots, f(x_{iD})] \tag{24}$$

Where $i = 1, 2, \cdots, N$ represents the number of sparrows in the population; $d = 1, 2, \cdots, D$ represents the number of design variables in the optimization problem.

In SSA, explorers have a wider search range, so they will prioritize obtaining food sources during the search process. In each iteration, the position update of the explorer is described as:

$$x_{id}^{t+1} = \begin{cases} x_{id}^t \cdot \exp\left(-\dfrac{i}{\alpha \cdot iter_{\max}}\right) & R_2 < ST \\ x_{id}^t + Q \cdot L & R_2 \geq ST \end{cases} \tag{25}$$

Where t is the current iteration count, $iter_{\max}$ is the maximum iteration count, $\alpha \in (0,1]$ is a randomly selected value, Q is a random number following a normal distribution, L is a $1 \times d$ matrix with all elements equal to 1, $R_2 \in [0,1]$ is the warning value, and $ST \in [0.5,1]$ is the safety value. When $R_2 < \mathrm{ST}$, it indicates that there are no predators in the environment, and the explorer can conduct a wide search. When $R_2 < \mathrm{ST}$, it indicates that the warning agent has detected a predator and issued an alert, at which point all sparrows will move to a safe area to forage [21].

Except for the explorers, all other sparrows in the population are followers. The position update iteration formula for followers is:

$$x_{id}^{t+1}=\begin{cases}Q\cdot\exp\left(\dfrac{x_{worst}^{t}-x_{id}^{t}}{i^{2}}\right) & i>\dfrac{N}{2}\\ x_{p}^{t+1}+\left|x_{id}^{t}-x_{p}^{t+1}\right|\cdot A^{+}\cdot L & others\end{cases} \tag{26}$$

Among these, x_{worst} represents the position of the globally worst solution, x_p is the optimal position of the current discoverer. When $i>N/2$, it indicates that the fitness value of the i th follower is low, there is a lack of food, and it is urgent to fly to another place to forage. When $i\leq N/3$, it indicates that the i th follower will forage near the optimal position. $A^{+}=A^{T}\left(AA^{T}\right)^{-1}$ where A is a $1\times d$ matrix with matrix elements randomly assigned values of 1 or -1.

Sparrows are randomly selected from the population as early warning agents, typically accounting for 10% to 20% of the population. The position updates for early warning agents are described as follows:

$$x_{id}^{t+1}=\begin{cases}x_{best}^{t}+\beta\cdot\left|x_{id}^{t}-x_{best}^{t}\right| & f_i>f_g\\ x_{id}^{t}+K\cdot\left(\dfrac{\left|x_{id}^{t}-x_{worst}^{t}\right|}{(f_i-f_w)+\varepsilon}\right) & f_i=f_g\end{cases} \tag{27}$$

Among them, x_{best} is the current global optimal solution position, β follows a standard normal distribution and is used to adjust the search step size, $K\in\left[-1,1\right]$ is randomly selected, f_i, f_w, and f_g are the current fitness values of the sparrow individuals, the current global worst fitness value, and the best fitness value, respectively, and ε is a very small constant to avoid the denominator being 0.

III. B. ISSA Algorithm and Model Solution

III. B. 1) Improving the Sparrow Search Algorithm

The SSA algorithm is widely used in solving complex optimization problems due to its superior performance, fast convergence speed, and few parameters. However, it still has drawbacks such as being prone to getting stuck in local optima. To enhance the overall capabilities of the SSA algorithm, this paper proposes an ISSA algorithm that integrates multiple strategies.

(1) Logistic Chaos Initialization Population Strategy

The Logistic chaos map is a typical representative of chaos maps. Due to the randomness and ergodicity of chaos, it can enhance the diversity of the initial population. Therefore, this paper applies the Logistic chaos map to the initialization of the SSA population, with its mathematical expression being:

$$X_{n+1}=uX_n\left(1-X_n\right) \tag{28}$$

In the equation, Y_n is the value generated by the n th generation of the chaotic sequence, and $Y_n\in\left[0,1\right]$, where u is the bifurcation parameter. When $3.57\leq u\leq 4$, the system is in a fully chaotic state, and when u is set to 4, better results are obtained with a more uniform population distribution. Therefore, this paper takes $u=4$.

The chaotic variables generated by the above equation are loaded into the solution space to be solved, i.e.:

$$X_{i,j}^{k}=X_{\min}+\left(X_{\max}-X_{\min}\right)\cdot X \tag{29}$$

In the equation, $X_{i,j}^{k}$ represents the initial position, and $X_{\max}$ and $X_{\min}$ represent the maximum and minimum values in the j th dimension, respectively.

(2) Introduction of the sine-cosine strategy

To address the slow convergence speed of the SSA algorithm, this paper introduces the sine-cosine algorithm (SCA) into the location update formula of the discoverer, applying the oscillatory characteristics of the sine-cosine model to the updated location of the discoverer to enhance the global search capability of the SSA algorithm. The basic sine-cosine algorithm's step size search factor formula is:

$$r_1=a-ar/iter_{\max} \tag{30}$$

In the equation, a is a constant, set to 1 in this paper, r is the current iteration count, and $iter_{\max}$ is the maximum iteration count. The step size search factor r_1 decreases linearly.

To better optimize the SSA algorithm, this paper divides the step size search factor into two parts: the first part is used for optimization in the early stage of the SSA algorithm, and the second part is used for optimization in the late stage of the SSA algorithm. The step size search factor formulas used for early optimization and late optimization are as follows:

$$r_1' = \alpha \times \left[1 - \left(\frac{r}{iter_{\max}}\right)^{\eta}\right]^{1/\eta} \tag{31}$$

$$r_1'' = \frac{e^{\frac{t}{iter_{\max}}} - 1}{e - 1} \tag{32}$$

In the formula, η is the adjustment coefficient, $\eta \geq 1$, $\alpha = 1$, and $iter_{\max}$ is the maximum number of iterations.

By introducing the step size search factor of the above optimization into SSA, we obtain the new discoverer position update formula:

$$G_{i,k}^{t+1} = \begin{cases} r_1'' G_{i,k}^t + r_1' \sin r_2 \cdot \left| r_3 \cdot G_{best}^t - G_{i,k}^t \right| & if \ Ra < TH \\ r_1'' G_{i,k}^t + r_1' \cos r_2 \cdot \left| r_3 \cdot G_{best}^t - G_{i,k}^t \right| & if \ Ra \geq TH \end{cases} \tag{33}$$

In the formula, $r_2 \in [0, 2\pi]$ is a random number representing the distance moved by the sparrow, and $r_3 \in [0, 2]$ is a random number representing the degree of influence of the optimal position on the next position.

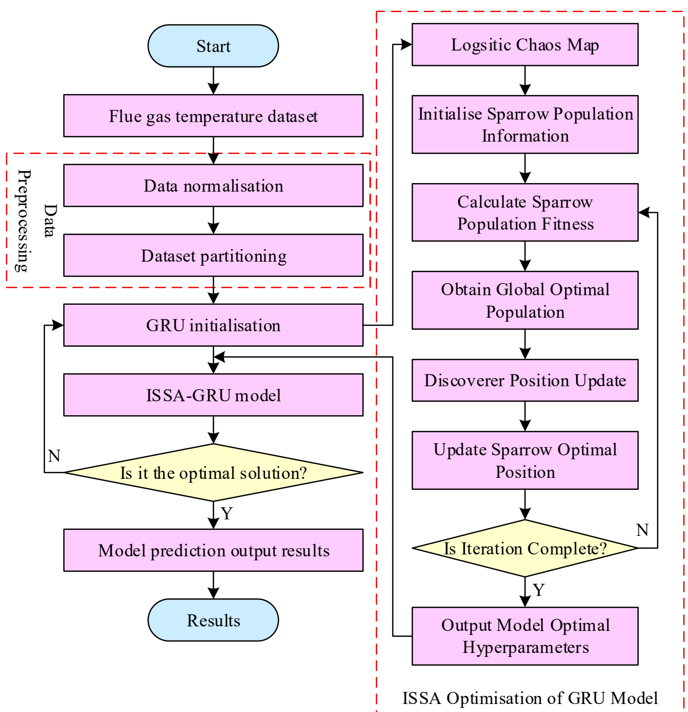

Figure 2: Flowchart of ISSA-GRU prediction model

III. B. 2) Optimizing the model solution process

Addressing the issues of manual parameter adjustment required for previous hospital spatial layout optimization and clinical risk prediction models, which led to poor model performance and overfitting, this paper proposes the ISSA-GRU combined prediction model. First, the collected hospital spatial layout and patient clinical medical data are preprocessed and divided into test and training sets to build the ISSA-GRU prediction model. Next, the ISSA-

GRU prediction model is trained using training samples. The ISSA algorithm is used to optimize hyperparameters such as the number of hidden layer neurons, learning rate, and iteration count in the GRU model. The mean squared error is used as the fitness metric for iterative optimization, resulting in the construction of the ISSA-GRU combined model. The workflow of the hospital spatial layout optimization and clinical risk prediction model based on ISSA-GRU is shown in Figure 2.

The specific steps are as follows:

Step 1 Data preprocessing. To avoid excessive numerical differences, the data is normalized and the dataset is divided into training and test sets.

Step 2 Build the initial GRU model. Set the number of layers and activation functions for the GRU grid structure.

Step 3 Population initialization. Initialize the population using the Logistic chaos map, calculate the fitness of the sparrow population, and obtain the current global optimal position.

Step 4 Introduce the cosine strategy to update the explorer's position, obtain the optimal position parameters, and update the current global optimal position.

Step 5 Determine whether the termination condition is met. Output the hyperparameters of the optimal model.

Step 6 Use the parameters optimized by ISSA to construct the GRU model training network.

Step 7 Train and predict the ISSA-GRU model using the hospital spatial layout and patient visit dataset, and evaluate the model's accuracy using error evaluation metrics.

IV. Optimization of hospital space layout and clinical risk management

With China's rapid urbanization process, the material living standards of the people have improved, directly driving the continuous growth in demand for high-quality medical services. Residents not only pursue improvements in medical technology and service quality, but also expect a more convenient and efficient experience when seeking medical treatment. As a key component of the urban public service system, the evolution of hospital architecture and functional layout has become an inevitable trend in response to this demand.

IV. A. Validation of the effectiveness of the ISSA-GRU algorithm

IV. A. 1) Effectiveness of the ISSA algorithm

To solve the hospital spatial layout optimization model, this paper designed the ISSA-GRU model and verified the effectiveness of the improved Sparrow Search Optimization Algorithm. Four different types of test functions were selected to evaluate the performance of the ISSA algorithm, and ablation experiments and comparison experiments were conducted. To ensure the validity of the tests, the runtime environments for all algorithms were set to be identical: population size of 60, maximum iteration count of 500, and individual dimension of 50. To ensure the reliability of the experiments and the accuracy of the data, each algorithm was run 50 times, and the average values were calculated. The results of the optimization solutions for the test functions by each algorithm are shown in Table 1.

As shown in the table, the ISSA algorithm based on the hybrid strategy demonstrated the best optimization performance compared to other algorithms in experiments involving the Sphere, Ackley, Griewank, and Rastrigin test functions, with both the average and optimal values consistently converging to the global optimal solution. The Logistic chaotic map enhances the randomness of the Markov process, thereby expanding the population's distribution range and enabling it to handle more complex search spaces. After introducing the cosine strategy, the algorithm performed exceptionally well on the Sphere, Griewank, and Rastrigin test functions, as it can balance the weights of global and local search during the search process, overcoming the effects of linear weights. In the test results for the Sphere and Ackley functions, the ISSA algorithm has the lowest standard deviation, indicating better stability and consistency. The optimal solution of the ISSA algorithm is close to the theoretical optimal solution, indicating that this algorithm has higher convergence accuracy compared to other algorithms. In the Griewank and Rastrigin functions, SSA-related algorithms can stably search for the optimal solution, indicating that SSA-related algorithms have higher adaptability to these two functions. Although the SSA algorithm can find the global optimal solution, its standard deviation is higher than that of SSA-related algorithms, indicating that the ISSA algorithm has higher robustness. In summary, compared with the comparison algorithms, the ISSA algorithm based on a hybrid strategy has higher optimization accuracy and faster convergence speed. Its application in GRU model parameter optimization is feasible and can provide support for hospital spatial layout optimization and clinical risk prediction.

Table 1: The effectiveness of the ISSA algorithm

Function	Algorithms	Means	SD	Optimal value	Worst value
Sphere	SSA	1.45*10-31	4.85*10-31	1.33*10-36	2.81*10-28
	SSA-Log	6.36-10-29	3.86*10-29	4.61*10-26	2.41*10-26

	SSA-SCA	0.000	0.000	0.000	0.000
	PSO	167.38	93.104	30.21	425.39
	GWO	2.18-10-42	5.46*10-42	2.65*10-43	3.41*10-38
	ISSA	0.000	0.000	0.000	0.000
Ackley	SSA	1.51*10-13	8.04*10-16	7.56*10-16	3.96*10-13
	SSA-Log	1.85*10-13	6.94*10-16	7.56*10-16	3.21*10-13
	SSA-SCA	4.42*10-15	0.000	4.42*10-16	4.42*10-16
	PSO	6.421	4.812	2.834	19.936
	GWO	2.83*10-13	3.01*10-16	2.15*10-13	3.24*10-13
	ISSA	4.42*10-18	0.000	4.42*10-18	4.42*10-18
Griewank	SSA	0.000	0.000	0.000	0.000
	SSA-Log	0.000	0.000	0.000	0.000
	SSA-SCA	0.000	0.000	0.000	0.000
	PSO	2.812	1.032	1.424	5.546
	GWO	5.01*10-4	8.05*10-3	0.000	0.031
	ISSA	0.000	0.000	0.000	0.000
Rastrigin	SSA	0.000	0.000	0.000	0.000
	SSA-Log	0.000	0.000	0.000	0.000
	SSA-SCA	0.000	0.000	0.000	0.000
	PSO	127.935	24.618	61.759	180.93
	GWO	0.386	1.327	5.63*10-15	6.275
	ISSA	0.000	0.000	0.000	0.000

IV. A. 2) Comparison of the performance of multiple models

To evaluate the effectiveness of the ISSA-GRU model designed in this paper for hospital spatial layout optimization and clinical risk management prediction, multiple different models were selected for performance comparison and evaluation. The evaluation metrics used include root mean square error (RMSE), mean absolute error (MAE), MAPE, and coefficient of determination (R^2). First, calculations were performed under different conditions, including varying numbers of hidden layer nodes, different numbers of input samples per iteration, and different training iterations, while simultaneously calculating the evaluation metrics for each parameter setting. Table 2 presents the prediction results of the ISSA-GRU model under different hyperparameter settings.

As shown in the table, the comparison results indicate that the model performs best when the number of hidden layer nodes is set to 40. When the number of hidden layer nodes is set to 40, comparing different input sample sizes shows that the model performs best when the number of samples input per iteration is 15. Further, when the number of hidden layer nodes is set to 40, the number of input samples per iteration is set to 15, and the number of training iterations is set to 400, the model performs best. Therefore, in the subsequent analysis, the number of hidden layer nodes, the number of input samples, and the number of training iterations for the ISSA-GRU model are set to 40, 15, and 400, respectively, to ensure that the model achieves optimal performance.

Table 2: Prediction of different super parameters

Hidden layer nodes	Sample quantity	Training rounds	MAPE	MAE	RMSE	R2
16	6	100	2.474	0.427	0.724	0.925
24	9	200	2.513	0.412	0.756	0.923
32	12	300	2.489	0.386	0.703	0.928
40	15	400	2.261	0.367	0.665	0.934
48	18	500	2.396	0.382	0.787	0.927
56	21	600	2.428	0.461	0.736	0.923
64	24	700	2.375	0.439	0.781	0.928

To further validate the effectiveness of the model proposed in this paper, LSTM, GRU, BiLSTM, and BiGRU models were selected as comparators. The prediction values of the aforementioned models were compared with the actual values to analyze the errors, with the specific results shown in Table 3. As can be seen from the data in the table, the ISSA-GRU model performs the best, with MAE and RMSE values of 0.224 and 0.326, respectively. Compared to the LSTM model, this represents improvements of 17.34% and 23.83%, and compared to the GRU model, improvements of 16.42% and 21.45%. After introducing the improved Sparrow Search Algorithm to optimize the traditional GRU neural network, the model performance has been enhanced. The ISSA-GRU model achieves a data fitting effect (R^2) of 0.916, which is 6.02%, 4.69%, 3.97%, and 3.27% higher than the other four models, respectively. Therefore, the ISSA-GRU model can more effectively uncover hidden information within the data, more accurately solve hospital spatial layout optimization issues, and effectively predict hospital clinical risk management outcomes, providing a more reliable basis for ensuring patient safety and enhancing the effectiveness of clinical risk prediction and early warning systems.

Table 3: Comparison of model performance

Model	MAPE/%	MAE	RMSE	R2/%
LSTM	2.875	0.271	0.428	0.864
GRU	2.791	0.268	0.415	0.875
BiLSTM	2.814	0.277	0.407	0.881
BiGRU	2.729	0.262	0.389	0.887
ISSA-GRU	2.208	0.224	0.326	0.916

IV. B. Analysis of the effects of optimizing hospital spatial layout

IV. B. 1) Effects of spatial layout optimization

Before using AnyLogic software for simulation modeling, according to the research purpose, certain assumptions and explanations are made on the system to simplify the model, so as to reduce the difficulty of establishing the simulation model and reduce the interference of irrelevant factors. Specifically, in order to simplify the spatial state of the patient, the patient was simplified into a two-dimensional circle, which was set to (0.3, 0.4) m. To further simplify the flow of patients, other flow lines of patient behavior in the channel are not considered. Patients take the shortest route to reach their destination, without asking others, and there is no turning back.

First, import the hospital's floor plan into AnyLogic software. Use spatial marking modules from the patient library, such as walls, target lines, rectangular areas, service lines, and paths, to draw the boundaries of the hospital's outpatient area, entrances/exits, self-service ticket machines, waiting queues, blood draw windows, and other environmental elements. Based on the spatial layout optimization strategy outlined earlier, the facility configuration and floor plan were optimized and adjusted in the AnyLogic software. Finally, the simulation model was rerun, and the optimized waiting area-time curve and patient dwell time curve are shown in Figures 3 and 4, respectively.

As shown in the figures, there is a significant change in the peak number of people in the hospital waiting area before and after optimization. After applying the spatial layout optimization strategy designed in this paper, the peak number of people fluctuates between 10 and 26. Before optimization, the peak number of people fluctuated between 35 and 50. Additionally, the average waiting time in the optimized waiting area is only about 24 people, a reduction of 41.46% compared to the 41 people before optimization. Furthermore, comparing the patient dwell time curves before and after optimization, the average dwell time after optimization is 15.78 minutes, a reduction of 35.62% compared to the 24.51 minutes before optimization. In summary, by leveraging the hospital spatial layout optimization strategy outlined in this paper and combining it with AnyLogic software, hospital spatial layout optimization can be achieved. Through relevant spatial layout optimization measures, the spatial congestion in the hospital waiting area can be effectively improved, ensuring patient safety and reducing patient dwell time.

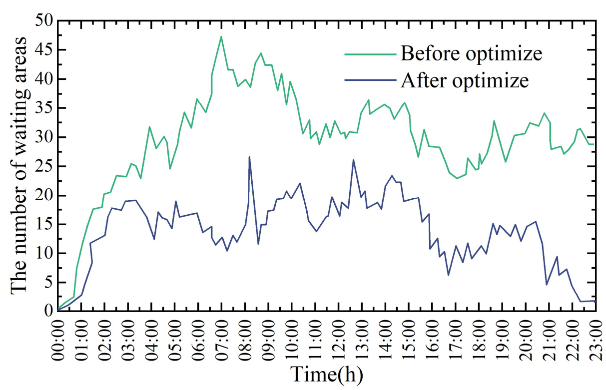

Figure 3: The waiting area of the waiting zone after optimization

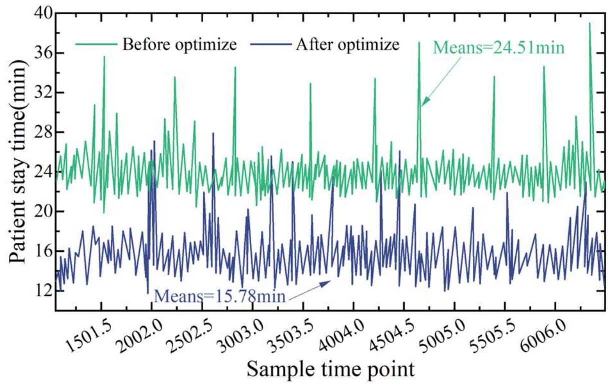

Figure 4: Optimize the time curve of the latter's stay

IV. B. 2) Evaluation of spatial layout optimization

The purpose of establishing a hospital spatial layout optimization and clinical risk prediction model in this paper is to further ensure patient safety during the hospital visit process, specifically by analyzing the convenience, safety, and rationality of the layout flow. Based on this, this paper introduces three indicators—passenger density, waiting time, and infection risk—to evaluate spatial layout optimization schemes. Passenger density refers to the average value of passenger density within a marked area during the simulation time. A higher result indicates more severe bottlenecks in the flow lines. Queueing time refers to the average time spent by a patient from joining the queue, through the registration/blood draw/medication pickup process, to leaving the registration/blood draw/medication pickup area, with higher results indicating greater convenience for patients. Infection risk refers to the contact time when a patient enters the current individual's 0.8-meter radius, starting from the time of contact until the patient leaves, i.e., the probability of infection.

Combined with the results obtained from the basic experiments, the overall passenger flow density of the hospital waiting point is low, but the density of self-service facilities is extremely high, which is likely to cause passenger congestion. According to the proposed spatial layout optimization scheme, the simulation model was adjusted and simulation experiments were carried out. The performance indicators of the optimization scheme are calculated, and the specific results are shown in Figure 5, where Figure 5 (a) ~ (c) are the experimental results of passenger flow density, queuing time and infection risk, respectively.

As shown in the figure analysis, the optimization scheme demonstrates significant improvements compared to the original scheme in terms of waiting time, passenger density, and infection risk.

(1) In terms of passenger density, the optimized scheme reduces passenger density by 19.51% to 63.16% compared to the original scheme across all service facilities. The high-density areas in the original scheme were primarily concentrated around the self-service facilities at the entrance of the lobby. Therefore, increasing the number of self-service facilities in low-density areas significantly reduces overall passenger density.

(2) In terms of waiting time, the reduction in waiting time compared to the original plan ranges from 20.36% to 34.23%. The blood draw area has the longest queueing time, despite a reduction of 5.23 minutes. However, due to the complexity of the blood draw process, optimization potential is limited. Additional measures such as increasing blood draw stations or offering appointment services could be considered based on actual conditions. The addition of self-service facilities has reduced queueing times in the registration window area and self-service facility area by approximately 1.2 to 2.4 minutes, alleviating efficiency issues.

(3) In terms of infection risk, the optimized spatial layout plan has a lower overall infection risk (<2.0%) compared to the original plan. When the passenger density in the waiting area decreases, the total duration of potential contact is reduced, thereby lowering the infection risk.

Therefore, the hospital spatial layout optimization strategy designed in this paper can better ensure patient safety during visits, effectively reduce clinical infection risks for patients, and provide a solid foundation for better meeting patient needs.

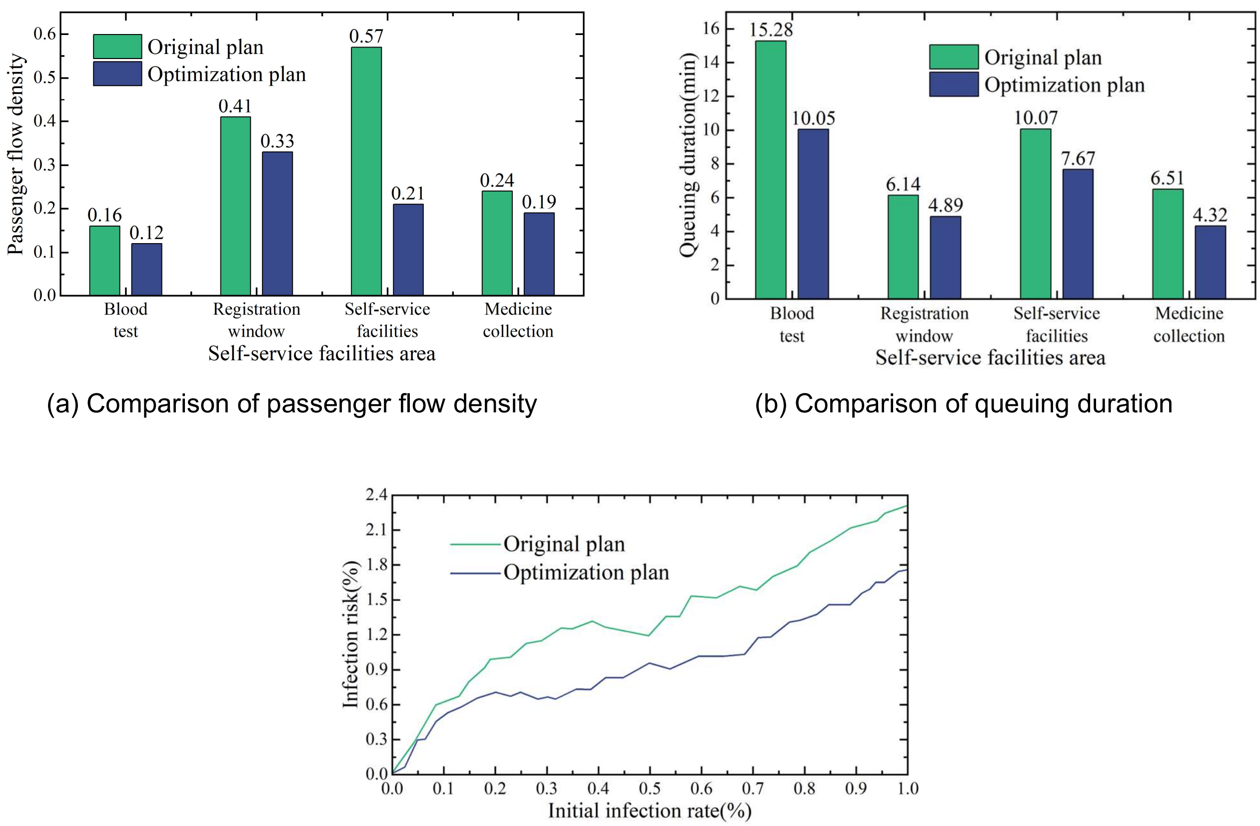

(a) Comparison of passenger flow density

(b) Comparison of queuing duration

(c) Comparison of infection risks

Figure 5: Evaluation of spatial layout optimization

V. Conclusion

The rational planning and allocation of medical facilities are crucial for enhancing the level of urban public services and promoting integrated urban-rural development. This paper establishes a hospital spatial layout and clinical risk prediction optimization model focused on patient safety, employs the ISSA-GRU model for solution, and conducts simulation analysis using AnyLogic software with a specific hospital as the research subject. Based on simulation data, the ISSA-GRU model designed in this paper demonstrates high performance, and the overall spatial layout optimization strategy is highly effective, significantly reducing hospital patient flow density and waiting times, thereby mitigating patient infection risks to a certain extent.

Although this study has achieved certain research results, there are still some shortcomings. For example, only one hospital was selected for simulation in the study, and the overall simulation model lacks representativeness. In future research, the study sample will be further expanded to construct a more universally applicable simulation model, thereby providing support for hospital spatial layout optimization and clinical risk management.

References

[1] Pan, M., Huang, Y., Qin, Y., Li, X., & Lang, W. (2022). Problems and strategies of allocating public service resources in rural areas in the context of county urbanization. International Journal of Environmental Research and Public Health, 19(21), 14596.

[2] LI, L., ZHOU, X., ZHAO, Y., & LU, Z. (2021). Degree of coordination between primary care resource allocation and economic development in eastern, central and western China. Chinese General Practice, 24(22), 2777.

[3] Chen, C. (2023). Discussion on the optimization method of public service facility layout from the perspective of spatial equity: A study based on the central city of Shanghai. Land, 12(9), 1780.

[4] Cubukcuoglu, C., Nourian, P., Tasgetiren, M. F., Sariyildiz, I. S., & Azadi, S. (2021). Hospital layout design renovation as a Quadratic Assignment Problem with geodesic distances. Journal of Building Engineering, 44, 102952.

[5] Chang, Y., Ai, Z., Wargocki, P., Liu, Y., & Hu, Y. (2024). Design of convertible patient care unit for both non-pandemic and pandemic times: Prototype, building spatial layout, and ventilation design. Building and Environment, 258, 111597.

[6] Wahyuningrum, S. H., & Wardhani, M. K. (2020). Efficiency of inpatient layout in private hospital (case study: bhakti asih hospital, brebes central java). Modul, 20(01), 1-9.

[7] Al Siwar, A. A., Alotayf, A. M. W., Almassabi, A. A., Haydar, H. M. S., Al Mansour, M. H. A., Almalki, S. A. H., ... & AlMtared, D. H. M. (2024). The Effect of Hospital Layout on Medication Safety Practices. Journal of International Crisis and Risk Communication Research, 7(S8), 700.
[8] Pachilova, R., & Sailer, K. E. R. S. T. I. N. (2019, July). Ward layout, communication and care quality: Spatial intelligibility as a key component of hospital design. In Proceedings of the 12th International Space Syntax Symposium. International Space Syntax Symposium.
[9] Xu, J., Peng, Y., Ye, C., Gao, S., & Cheng, M. (2024). Hospital Flow Simulation and Space Layout Planning Based on Low-trust Social Force Model. IEEE Access.
[10] Chen, X., Qiu, L., Ma, H., Jin, M., & Wang, M. (2024). Computer-aided hospital layout optimization based on patient flow analysis: A case study from China. Journal of Building Engineering, 88, 108899.
[11] Huang, X. (2024). Environmental Performance-Driven Parametric Design Method for General Hospitals Layout Design. Advances in Computer and Materials Scienc Research, 1(1), 321-332.
[12] Shi, Y., Li, Y., Wang, R., & Li, X. (2025). A framework for optimizing the indoor spatial layout of outpatient building focusing on respiratory infection control by improving natural ventilation. Journal of Building Engineering, 104, 112352.
[13] Kılıç, T., Bostan, S., & Şentürk, F. (2017). Risk management in healt institution: Risk analysis of a public hospital. Journal of International Health Sciences and Management, 3(4), 20-28.
[14] Michel, P., Brami, J., Chanelière, M., Kret, M., Mosnier, A., Dupie, I., ... & Quenon, J. L. (2017). Patient safety incidents are common in primary care: A national prospective active incident reporting survey. PLoS One, 12(2), e0165455.
[15] Li, H., Li, L., Liu, T., Tan, M., He, W., Luo, Y., ... & Sun, J. (2024). Risk management and empirical study of the doctor-patient relationship: based on 1790 litigation cases of medical damage liability disputes in China. BMC Health Services Research, 24(1), 521.
[16] Liang, W., Liang, H., Ou, L., Chen, B., Chen, A., Li, C., ... & He, J. (2020). Development and validation of a clinical risk score to predict the occurrence of critical illness in hospitalized patients with COVID-19. JAMA internal medicine, 180(8), 1081-1089.
[17] Bolcato, M., Fassina, G., Rodriguez, D., Russo, M., & Aprile, A. (2019). The contribution of legal medicine in clinical risk management. BMC Health Services Research, 19, 1-6.
[18] Fauer, A., Wright, N., Lafferty, M., Harrod, M., Manojlovich, M., & Friese, C. R. (2021). Influences of physical layout and space on patient safety and communication in ambulatory oncology practices: A multisite, mixed method investigation. HERD: Health Environments Research & Design Journal, 14(4), 270-286.
[19] Ramya Chinnasamy,Malliga Subramanian,Nandita Sengupta & Ramkumar MP. (2025). Contextual Internet of Things Intrusion Detection: A Sliding Window Convolutional Neural Network–Gated Recurrent Unit Model Enhanced by Graph Neural Networks. Cureus Journal of Computer Science,2(1),6001-6001.
[20] Sakorn Mekruksavanich,Wikanda Phaphan & Anuchit Jitpattanakul. (2025). Sensor-Based Hand Gesture Recognition Using One-Dimensional Deep Convolutional and Residual Bidirectional Gated Recurrent Unit Neural Network. Lobachevskii Journal of Mathematics,46(1),464-480.
[21] Yongmei Wang,Junyong Li & Xiaoyun Tan. (2025). Chaos and elite reverse learning – Enhanced sparrow search algorithm for IIoT sensing communication optimization. Alexandria Engineering Journal,125,663-676.